

MicroPhaseNO: Adapting an Earthquake-Trained Phase Neural Operator for Microseismic Phase Picking

Ayrat Abdullin^{1*}, Umair bin Waheed^{1*}, Leo Eisner² and Naveed Iqbal³

^{1*}Department of Geosciences, King Fahd University of Petroleum and Minerals, Dhahran, 31261, Saudi Arabia.

²Seismik s.r.o., Kubišova 8, Praha, 18200, Czechia.

³Department of Electrical Engineering, King Fahd University of Petroleum and Minerals, Dhahran, 31261, Saudi Arabia.

*Corresponding author(s). E-mail(s): g202203180@kfupm.edu.sa;
umair.waheed@kfupm.edu.sa;

Contributing authors: leo@seismik.cz; naveediqbal@kfupm.edu.sa;

Abstract

Seismic phase picking is very often used for microseismic monitoring and subsurface imaging. Traditional manual processing is not feasible for either real-time applications or large arrays. Deep learning-based pickers trained on large earthquake catalogs offer an automated alternative. However, they are typically optimized for high signal-to-noise, long-duration networks and struggle with the challenges presented by microseismic datasets, which are purpose-built for limited time without previously detected seismicity.

In this study, we demonstrate how a network-wide earthquake phase picker, the Phase Neural Operator (PhaseNO), can be adapted to microseismic monitoring using transfer learning. Starting from a PhaseNO model pre-trained on more than 57,000 three-component earthquake and noise records, we fine-tune the model using only 200 labeled and noise seismograms from induced events in hydraulic-fracturing settings. The fine-tuned model thus preserves the rich spatio-temporal representation learned from abundant earthquake data, while adapting to the characteristics and labeling conventions of microseismic phases, which are often picked on peaks or troughs rather than onsets.

We evaluate performance on three distinct real-world microseismic datasets with different network geometries and acquisition parameters. Compared to the original PhaseNO and a conventional workflow, the adapted model increases F1 score and accuracy by up to 30%, and strongly reduces systematic timing bias and pick uncertainty. Because the adaptation relies on a small, campaign-specific calibration set, the approach is readily transferable to other microseismic tasks where public earthquake data and pre-trained models are accessible. The associated code will be released openly at <https://github.com/ayratabd/MicroPhaseNO>.

Keywords: microseismic monitoring, induced seismicity, phase picking, neural operators, transfer learning, machine learning

1 Introduction

Earthquake detection and localization are critical for real-time monitoring of induced seismic activity. Although coarse locations can be obtained by using single-station phase picking algorithms, based, for example, on skewness and kurtosis (Baillard et al. 2014), achieving accurate locations requires either manual picking or automated algorithms using a picking association across the whole network of receivers. Traditionally, seismologists have visually inspected waveforms across multiple stations to manually pick the P- and S-wave arrivals. This process is inherently subjective, labor-intensive, and error-prone.

Recent advances in neural network-based approaches have significantly enhanced phase-picking efficiency (Ross et al. 2018; Zhu and Beroza 2019; Mousavi et al. 2020; Baker et al. 2021; Feng et al. 2022; Shi et al. 2024). These published algorithms are often used in their original form (Van der Laat et al. 2021; Retaillieu et al. 2022) or after being fine-tuned with custom training datasets (Chai et al. 2020; Armstrong et al. 2023). For instance, Ross et al. (2018) developed a convolutional neural network (CNN) on a carefully studied Southern California Seismic Network dataset to accurately determine arrival times and polarity of the P waves, outperforming expert seismologists. Zhu and Beroza (2019) presented PhaseNet, a fully convolutional network that robustly detects both P- and S-wave arrivals under complex conditions. Wang et al. (2019) achieved state-of-the-art results with a CNN trained on high-sensitivity, three-component data from Japan. Chai et al. (2020) leveraged transfer learning from natural earthquake datasets to improve phase picking in laboratory hydraulic fracturing experiments. More recently, Zhou et al. (2025) introduced AI-PAL that combines a Self-Attention recurrent neural network with PAL rule-based detections (phase Picking - phase Association - event Location). Generally, the CNN algorithm uses multiple components to identify phase arrivals and improve detection completeness, phase association rates, and processing speed compared to manual picking. These algorithms use high signal-to-noise ratio (SNR) waveforms of strong earthquakes and are applied to stationary networks for which the training dataset is acquired on the same network as it is used to validate

and test. However, microseismicity poses unique challenges (Anikiev et al. 2023): low SNR events and variable monitoring networks with no prior recorded seismicity.

Deep learning algorithms were also applied to mining and microseismic data, including neural network architectures alternative to CNNs. For example, sequence models such as LSTM were used for arrival picking by Kirschner et al. (2019), demonstrating the effectiveness of local earthquake classification. He et al. (2020) employed capsule networks for P-waves detection in copper mine monitoring, achieving better generalization with fewer training samples than CNNs. Johnson et al. (2021) adapted Ross et al.’s CNN algorithm (Ross et al. 2018) for microseismic surveying of mining, showing improved performance after fine-tuning on a specific dataset. Kolar et al. (2023) developed an RNN-based phase picker, adapted for data from a local seismic monitoring array designed for the analysis of induced seismicity. Most machine learning (ML) phase-picking algorithms are based on single-station strategies, which may result in missed detection of low SNR events or false detection of local noise signals with emergent arrivals.

Recently, array-based arrival picking algorithms have been proposed that exploit the spatial seismic phase coherence across multiple stations. For example, Chen and Li (2022) demonstrated that the CubeNet model effectively suppresses local spurious noise that often compromises trace-based methods. Similarly, Feng et al. (2022) presented EdgePhase, a multi-station arrival picking algorithm integrating the Edge Convolutional module with EQTransformer. In comparison with the standard EQTransformer, EdgePhase demonstrated a 5% increase in F1 score (the weighted average of precision and recall) on the Southern California dataset. These advancements underscore the potential of array-based methods for more robust and generalizable phase picking.

In this paper, we build on these developments by leveraging the Phase Neural Operator (PhaseNO) (Sun et al. 2023) (Figure 1), a network-wide phase-picking algorithm based on the advanced Neural Operators framework (Kovachki et al. 2023). Designed to work with functions rather than finite-dimensional vectors, the neural operators learn mappings between function spaces and have become powerful tools

for modeling partial differential equations (PDEs) and in other scientific applications. By incorporating spatio-temporal context, PhaseNO is capable of simultaneously picking seismic phases across arbitrary network geometries. Hence, it has the potential to solve one of the two major challenges of microseismicity: detecting phase arrivals on variable non-stationary networks. Sun et al. (2023) applied the PhaseNO to a stationary network; we show how this methodology can be extended for new local networks with transfer learning.

We adapt and evaluate PhaseNO on real microseismic datasets, demonstrating that our fine-tuned model outperforms the original pre-trained version and conventional methods by achieving higher consistency with manual picks. This approach not only highlights the benefits of exploiting spatio-temporal information for seismic phase picking but also expands the potential for enhanced microseismic monitoring. Because large, high-quality earthquake phase-picking datasets are publicly available while comparably sized microseismic datasets are not, our strategy is to leverage a pre-trained PhaseNO model and adapt it to microseismic monitoring using only a small number of campaign-specific labeled microseismic events. In doing so, we also address a second challenge of microseismic monitoring: acquisition networks are typically purpose-built and deployed in regions with little or no prior recorded seismicity, in contrast to permanent earthquake monitoring networks. Our results show that PhaseNO can be effectively generalized to such purpose-built microseismic arrays, enabling reliable phase picking without the need to train a dedicated model from scratch for each new deployment.

2 Data

This study utilizes three real microseismic datasets, each characterized by significantly different monitoring array designs and seismicity features (Figure 2). The first dataset, D1, consists of approximately 600 triggered microseismic events recorded during hydraulic fracturing operations in British Columbia (Canada), along with manually picked P- and S-wave phase arrival times and the seismic catalog. The data were collected using nine three-component surface seismic sensors with a sampling rate of 250 Hz, deployed on a surface area of approximately 100 km². False events

are created by taking background seismic noise recording in time intervals without any detected seismicity from 24-hour continuous recordings on all the stations before the operations started.

The second dataset D2 consists of 39 triggered events recorded during hydraulic fracturing operations in Ohio (United States). The induced seismicity data were acquired with five three-component surface seismic stations with a sampling rate of 250 Hz, covering an area of approximately 25 km². As with D1, D2 has manually picked phase arrival times and an accompanying location catalog.

The third dataset (D3) comprises 20 triggered records acquired during industrial operations in the United States. The monitoring array consisted of eleven three-component surface stations sampling at 500 Hz, deployed across an area of approximately 800 km². The dataset includes an equal proportion of local seismic events and false triggers, providing a balanced set for evaluating event discrimination performance.

To ensure compatibility with the input dimensions required by the original PhaseNO model, seismograms from both datasets were resampled to 100 Hz and divided into 30-second segments (each comprising 3000 samples). The final utilized dataset comprised 1,460 waveform segments derived from approximately 650 labeled seismic triggers, representing both local and near-field events, which are typically located at least 10 km from the nearest station.

3 Methodology

We employ the Phase Neural Operator (PhaseNO) model (Sun et al. 2023) as the core of our phase picking approach. The model uses two specialized neural operators to capture the intrinsic structure of seismic data. Temporal information is processed using layers of Fourier neural operators (FNO) (Li et al. 2020a), which use fast Fourier transforms to efficiently encode regularly sampled seismograms. Spatial information, on the other hand, is modeled using graph neural operators (GNO) (Li et al. 2020b), which use message passing (Gilmer et al. 2017) to aggregate features across irregularly distributed sensors. This dual approach ensures robust phase picking across varying seismic network configurations.

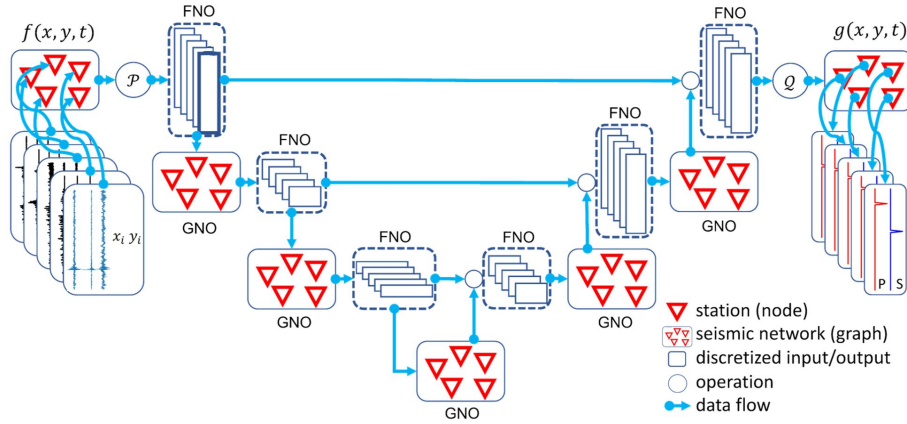


Fig. 1 The architecture of the Phase Neural Operator. The network is built from multiple layers of Fourier Neural Operators (FNO) and Graph Neural Operators (GNO) arranged sequentially and iteratively. The up and down projections, denoted by P and Q , respectively, are implemented using neural networks. The model processes seismograms collected from a seismic network with arbitrarily located stations and predicts the P-phase and S-phase arrival time probabilities for each station. In addition to the three channels containing the three-component waveforms, the station locations are encoded as two separate channels, and the relative coordinates (x_i, y_i) between stations are used to learn the edge weights in the graph (adapted after Sun et al. 2023).

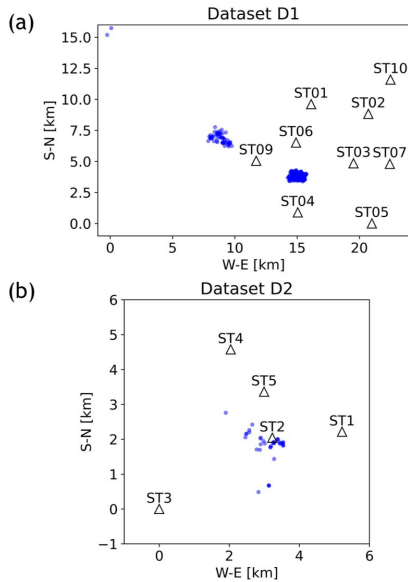


Fig. 2 The maps illustrate the locations of both datasets D1 (a) and D2 (b) with seismic stations and induced event epicenters. Network stations are marked with triangles. The events occur at an average depth of 2.1 km, ranging from 1.7 to 2.4 km (D1), and 3.1 km, ranging from 2.8 to 3.4 km (D2).

To further enhance performance on microseismic data, we developed a transfer learning (TL) workflow based on a pre-trained PhaseNO model originally trained on over 57,000 three-component seismic records from natural earthquakes in

Northern California (1984–2019) and noise waveforms from the STanford EArthquake Dataset (STEAD). Although the pre-trained model was designed for seismograms with source-receiver distances ranging from a few to tens of kilometers, it demonstrated reasonable performance on our microseismic datasets. Our objective was not to further improve the original earthquake PhaseNO model, but to transfer its learned, network-level representation to a microseismic regime with scarce labeled data. The fine-tuning step effectively re-calibrates the model to microseismic picking conventions (peaks/troughs), source receiver distances, stations placed in sedimentary basins and survey-specific noise characteristics, while preserving the information extracted from abundant earthquake datasets. We fine-tuned PhaseNO using a subset of our data that meets the original training requirements, i.e., normalized three-component seismograms with groundtruth P- and S-wave arrival times.

During TL, we retained the overall architecture of PhaseNO and initialized the weights with the pre-trained parameters. Our seismic events were partitioned into five sets:

- Training: 100 local and 100 false events from the 9-station dataset D1,

- Validation: 50 local events from the 5-station dataset D2 and 50 false events from D1 re-grouped to the D2 stations (5 random D1 stations),
- Testing (3 sets):
 - ◊ 500 local and 500 false events from D1,
 - ◊ 50 local events from D2 and 50 false events re-grouped from D1,
 - ◊ 10 local and 10 false events from the 11-station dataset D3.

No overlapping between the samples was ensured for all the local and false events. The training set was used to re-train the model, the validation set to adjust the learning rate and early stopping, and the test set to evaluate the performance. To account for labeling uncertainty, we used the probability density function in the shape of a triangle with a base of 0.4 sec, centered on the manual picks (same function used in the original paper).

The fine-tuning process was conducted using the AdamW optimizer with a learning rate of $5e-5$, a batch size of 1, and the ReduceLROnPlateau scheduler. The training objective was to maximize the overall F1 score (a harmonic mean of the precision and recall metrics). The training proceeded until the validation F1 score is not improved for 10 epochs (Figure 3).

We performed a cross-validation study with the same model hyperparameters only varying a set of trainable PhaseNO blocks (Figure 4). Each case involved 5 fine-tuning runs starting with the pre-trained weights. The study showed that the maximum validation F1 scores can be achieved with training on more PhaseNO blocks, and the best model was chosen from the run with all the layers trainable. Training from scratch with the same model architecture but starting with random weights did not reach even 20% for the F1 score. We then evaluated the performance of the fine-tuned model by comparing the predicted arrival times with human analysts’ picks, using key confusion matrix metrics to comprehensively assess detection performance.

Confusion matrix derived parameters include precision, recall, F1-score, and accuracy. Precision quantifies the proportion of correct detections out of all identified detections, while recall measures the model’s ability to capture known phase arrivals. The F1-score is defined as the harmonic

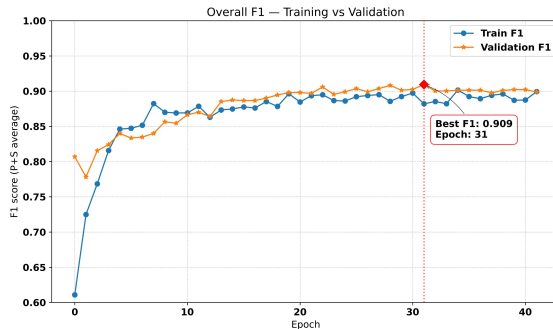


Fig. 3 Evolution of the average P- and S-phase F1 score during training. Shown are the training and validation F1 curves over 42 epochs, with the validation performance peaking at an F1 score of 0.85 at epoch 32. The divergence between the two curves after ≈ 20 epochs reflects progressive overfitting, whereas the early plateau in the validation curve indicates stabilization of generalization performance.

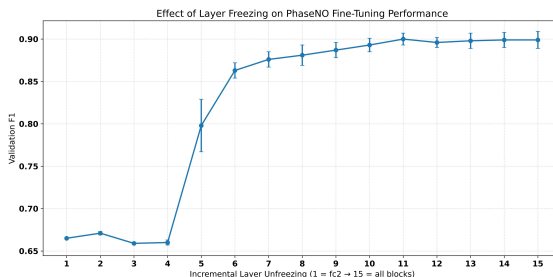


Fig. 4 Impact of progressive unfreezing of PhaseNO layers on validation F1 score. Each point represents the mean (± 1 SD) over five independent fine-tuning runs. Performance increases monotonically as deeper FNO/GNO blocks are unfrozen, with the first major gain occurring when the gno5 block is released. Optimal performance (F1 ≈ 0.845) is obtained when nearly all blocks are trainable, confirming that deep structural adaptation is essential for high-accuracy microseismic phase picking.

mean of precision and recall and provides a balanced metric that includes both false positives and false negatives. Accuracy is calculated as the ratio of correctly identified instances to the total number of observations. Together, these metrics provide an overall assessment of detector performance, balancing the need to minimize false alarms and maximize the detection of correct phase arrivals. Note, the confusion matrix derived metrics do not account for errors in the manually labeled data. The number of true positives, false positives, false negatives, and true negatives was computed for each station and then summed

for all events to get the final scores. The arrival time difference between manual and model picks was considered correct if it was less than the chosen threshold of 0.5 sec (same with the original PhaseNO paper).

4 Results and Discussion

By transfer learning, we overcome the difference in spatial scale between our microseismic data and the natural earthquake data used for original training. Thanks to this approach, fine-tuning the pre-trained model required only 200 seismograms ($200 / 57,000 = 0.4\%$ of the original training dataset), demonstrating the efficiency of this approach. The fine-tuned model achieved arrival time picking performance comparable to that of human analysts while significantly reducing the inference time for phase picking.

Quantitative evaluation using confusion matrix metrics further underscored the improvements brought by fine-tuning. For test set #1, the fine-tuned model demonstrated up to a 13-22% increase in precision, 5-9% in recall, 10-17% in F1 score, and 9-16% in overall accuracy relative to the original PhaseNO (Figure 5). Note that the original model achieved a good recall, but low precision and F1 scores, indicating approximately 20% failure without fine-tuning.

Similar improvements were observed in dataset D2 (Figure 5), which included a more sparse set (five stations compared to nine in D1), highlighting the ability to use the fine-tuned model on a new network, which was not used in the training. This advantage is of high importance for induced seismicity as it allows the use of sparse networks without prior induced seismicity detected on these networks. The confusion matrix scores for D3 were overall lower but still better by 30-40% than the original model.

To provide a benchmark against which to evaluate the machine-learning results, we implemented a classical picking workflow combining STA/LTA triggering and polarization analysis. P-wave arrivals were first identified on the vertical component using a short-term/long-term average (STA/LTA) detector, where exceedance of a predefined onset threshold marked the preliminary pick. This initial estimate was subsequently refined within a ± 0.5 -s window using the Akaike Information Criterion (AIC) to obtain a more

stable onset time. S-wave picking was performed on the three-component seismograms by scanning a sliding window and locating the time at which the horizontal-to-total energy ratio is maximized, constrained to occur after the P arrival and within a physically reasonable S-P interval. This hybrid STA/LTA-AIC P picker together with the polarization-based S picker represents a standard, physics-based baseline commonly used for comparison in local earthquake analysis. The results presented in Figure 6 confirm that machine-learning algorithms are more reliable than the conventional method employed.

Both the original and fine-tuned models were evaluated on a comprehensive test set comprising seismograms that were not used during training. Randomly selected waveforms and their corresponding picks from the test dataset show a strong agreement between the TL results and the manual labels, even in low SNR conditions (Figure 7).

Additionally, analysis of picking errors and predicted uncertainty intervals (Figures 8 and 9) revealed that the original model picks have more negative bias in the difference between manual and model picks, and the fine-tuned picks do not have such bias. This observation probably results from the fact that the original earthquake training dataset was picked on the onset of arrivals, while the microseismic datasets were picked on peaks/troughs of the arrivals. The second important observation is the smaller uncertainty in the fine-tuned model pick times, resulting in a narrower probability distribution around the correct time. The distribution of one-sigma confidence intervals is approximately three times as wide as that of the original model, indicating enhanced certainty in the phase arrival estimates. This behavior illustrates that the fine-tuned model is not simply ‘more accurate’ in a generic sense; rather, it has adapted from an onset-based earthquake labeling convention to a peak/trough-based microseismic convention, aligning its internal representation with the way microseismic analysts define phase arrival times.

We also compare how the model performance changes with varying the threshold for detecting true positives. Figure 10 illustrates that even with increasing the threshold value from 0.1 to 1 the original PhaseNO model F1 score remains smaller than the fine-tuned one.

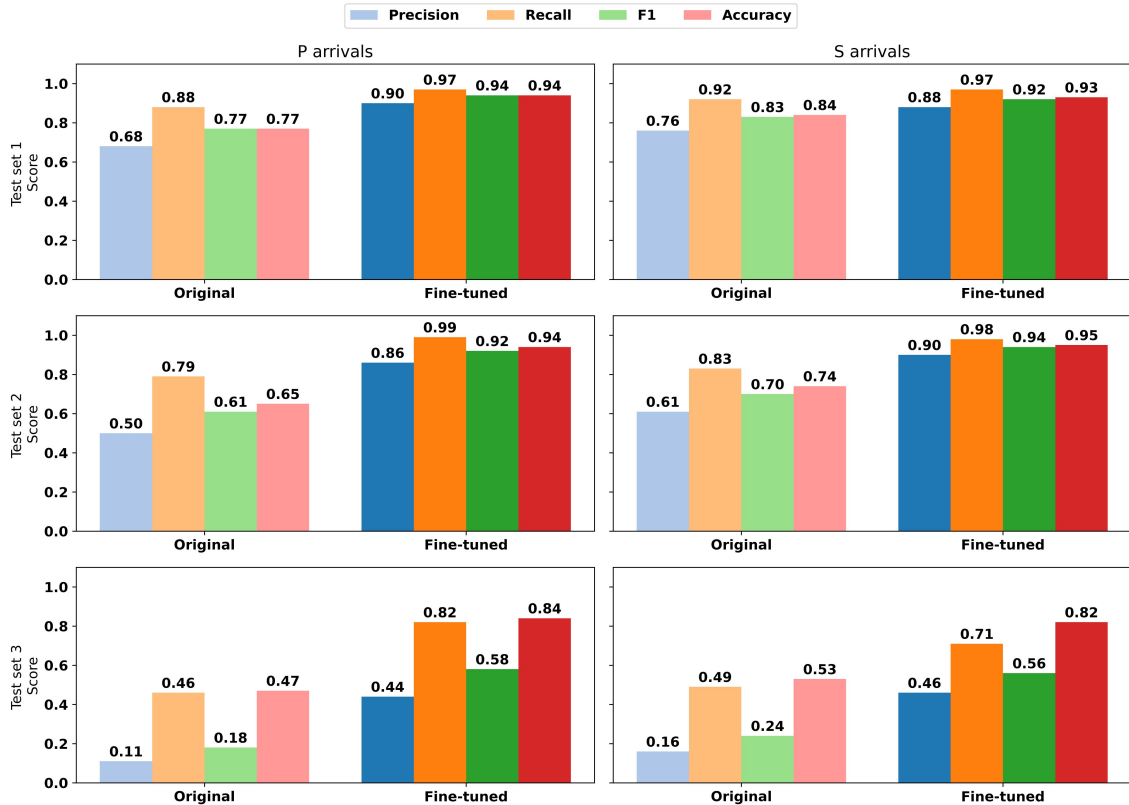


Fig. 5 A comparison of performance between the original PhaseNO and the fine-tuned model for P and S arrival picks for the three test sets. We use precision, recall, F1, and accuracy scores to quantify and compare the performance.

Thus, these results demonstrate that fine-tuning PhaseNO on microseismic data substantially refines phase arrival detection and uncertainty estimation, providing a robust, efficient solution for automated seismic monitoring and improving the characterization of induced seismic events.

5 Conclusions

Accurate phase picking is crucial for reliable seismic event detection and subsurface imaging.

In this study, we developed a transfer-learning framework that repurposes the earthquake-trained Phase Neural Operator (PhaseNO) for microseismic monitoring. Our goal was to adapt PhaseNO’s rich, network-level representation of seismic wavefields to the specific characteristics and constraints of induced microseismicity, where labeled data are scarce and acquisition geometries are survey-dependent.

Starting from a PhaseNO model trained on more than 57,000 three-component earthquake and noise records, we fine-tuned the model using only 200 microseismic and false-event seismograms, i.e., approximately 0.4% of the original training volume. This light-weight adaptation is sufficient to bridge key domain gaps, including differences in spatial scale, signal-to-noise ratio, and picking conventions. The original PhaseNO was trained on onset-based arrival times for regional earthquakes, whereas our microseismic labels correspond to peaks/troughs of arrivals. The fine-tuned model systematically reduces the negative timing bias observed in the original predictions and yields significantly narrower uncertainty intervals for both P and S picks, indicating that the model has been re-calibrated to the microseismic picking practice rather than merely overfitted to a small dataset.

Across three independent test sets with different network configurations and acquisition parameters, the adapted PhaseNO improves F1 scores

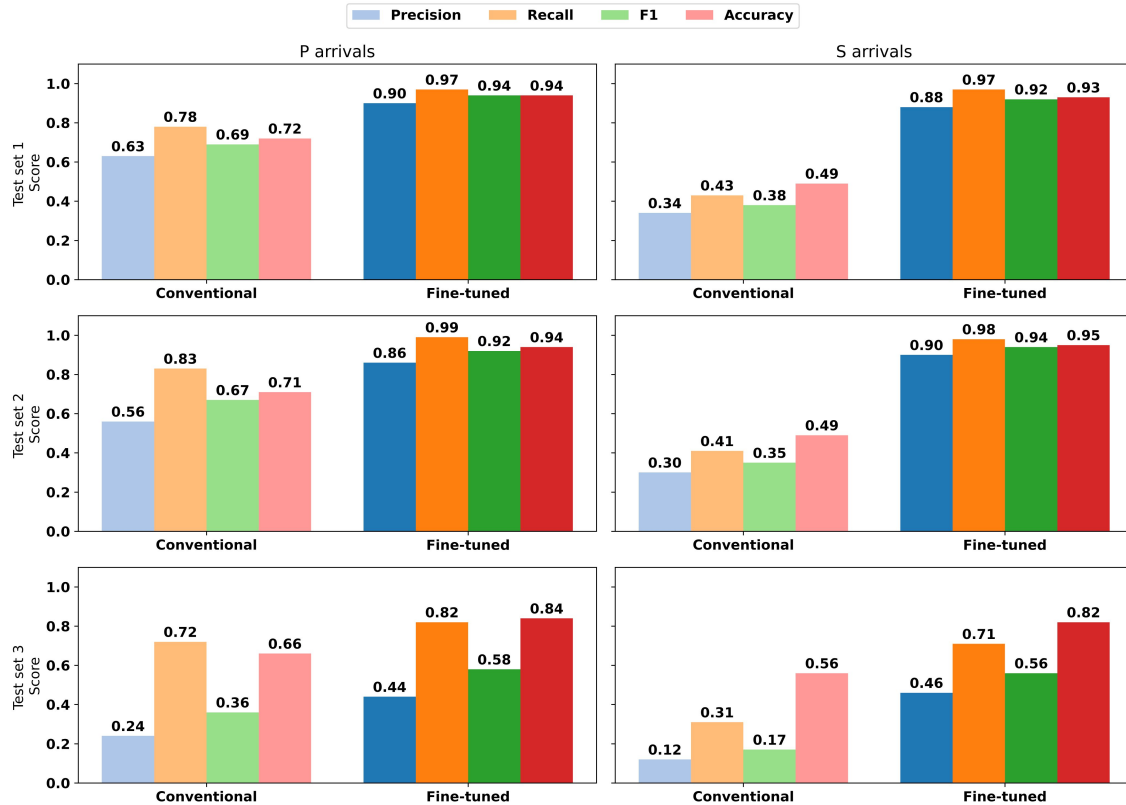


Fig. 6 A comparison of performance between the conventional STA/LTA method and the fine-tuned model for P and S arrival picks for the three test sets. We use precision, recall, F1, and accuracy scores to quantify and compare the performance.

by up to 30% relative to the pre-trained model, while also attaining considerable gains in precision, recall, and overall accuracy. It also outperforms a conventional STA/LTA–AIC P-picker combined with polarization-based S-picking, particularly for low-SNR events where array-level context is essential.

These results show that large public earthquake datasets and pre-trained multi-station models can be used as a foundation for robust microseismic phase picking, even when only a small number of survey-specific microseismic events are available for calibration. The proposed MicroPhaseNO workflow provides a cost-effective path to deploy state-of-the-art models in data-limited microseismic applications, reducing manual effort and helping to better characterize induced seismicity and the development of subsurface fractures.

Acknowledgment

We gratefully acknowledge the support of King Fahd University of Petroleum and Minerals (KFUPM) through the Outbound International Visiting Program grant no. ISP22210. We are extremely grateful to Prof. George Karniadakis and Dr. Khemraj Shukla from the Department of Applied Mathematics and Engineering at Brown University for useful discussions on neural operators.

Conflict of interests

On behalf of all authors, the corresponding author states that there is no conflict of interest.

Author contributions

Conceptualization: Umair bin Waheed; Data curation: Ayrat Abdullin, Leo Eisner; Formal analysis: Umair bin Waheed, Leo Eisner, Naveed

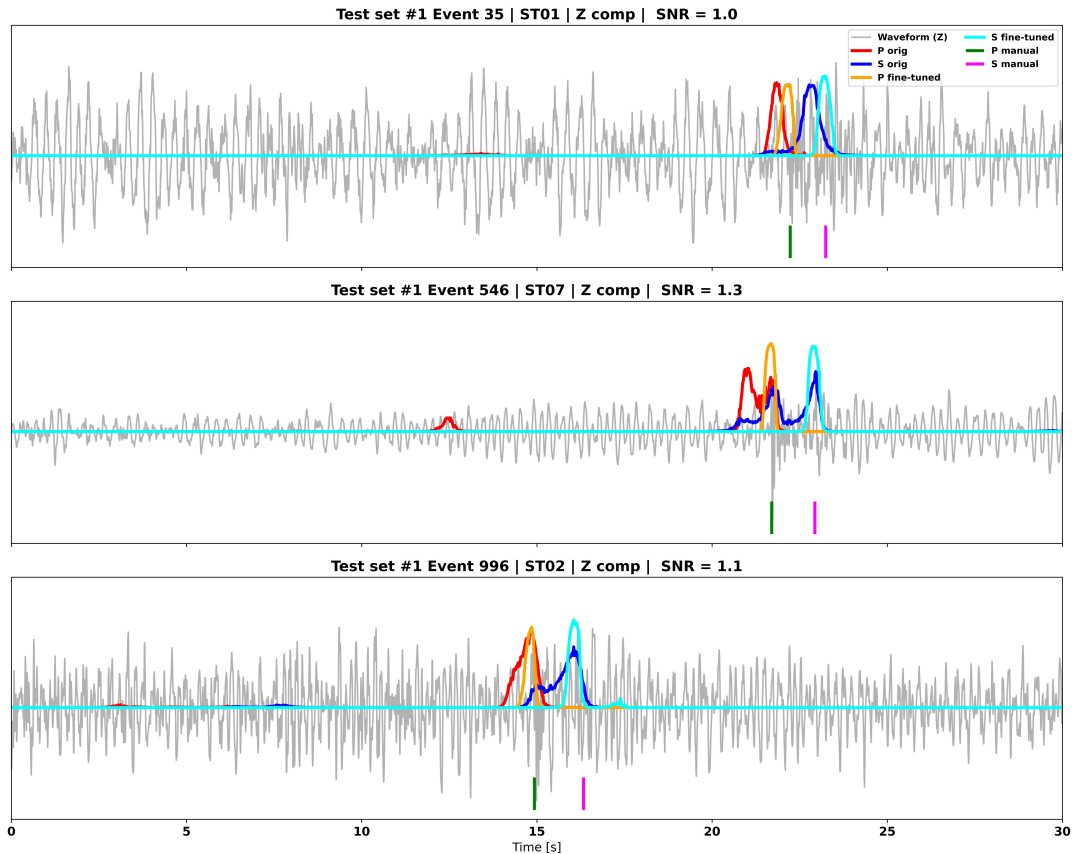


Fig. 7 Example waveforms from test set #1 illustrating the performance of original (red and blue curves) and fine-tuned (orange and cyan curves) PhaseNO models under varying signal-to-noise ratios (SNR). The red and orange curves represent P-pick probabilities, while the blue and cyan are S-pick probabilities. The green and magenta vertical lines denote manual picks of P- and S-wave arrivals, respectively. The fine-tuned model predictions align more closely with the manual picks, especially noticeable at lower SNR values, highlighting the improved robustness and accuracy achieved through transfer learning.

Iqbal; Methodology: Ayrat Abdullin, Umair bin Waheed, Leo Eisner; Project administration: Ayrat Abdullin; Resources: Umair bin Waheed, Leo Eisner; Supervision: Umair bin Waheed; Validation: Leo Eisner, Naveed Iqbal; Visualization: Ayrat Abdullin; Writing - original draft: Ayrat Abdullin; Writing - review and editing: Ayrat Abdullin, Umair bin Waheed, Leo Eisner, Naveed Iqbal.

Data availability

The microseismic datasets underlying this article were provided by Seismik s.r.o. to be used in this study. These datasets will be shared on request to the corresponding author with permission of Seismik s.r.o.

References

- Anikiev, D., Birnie, C., Waheed, U., Alkhali-fah, T., Gu, C., Verschuur, D.J., Eisner, L.: Machine learning in microseismic monitoring. *Earth-Science Reviews* **239**, 104371 (2023)
- Armstrong, A.D., Claerhout, Z., Baker, B., Koper, K.D.: A deep-learning phase picker with calibrated bayesian-derived uncertainties for earthquakes in the yellowstone volcanic region. *Bulletin of the Seismological Society of America* **113**(6), 2323–2344 (2023)
- Baillard, C., Crawford, W.C., Ballu, V., Hibert, C., Mangeney, A.: An automatic kurtosis-based p-and s-phase picker designed for local seismic networks. *Bulletin of the Seismological Society*

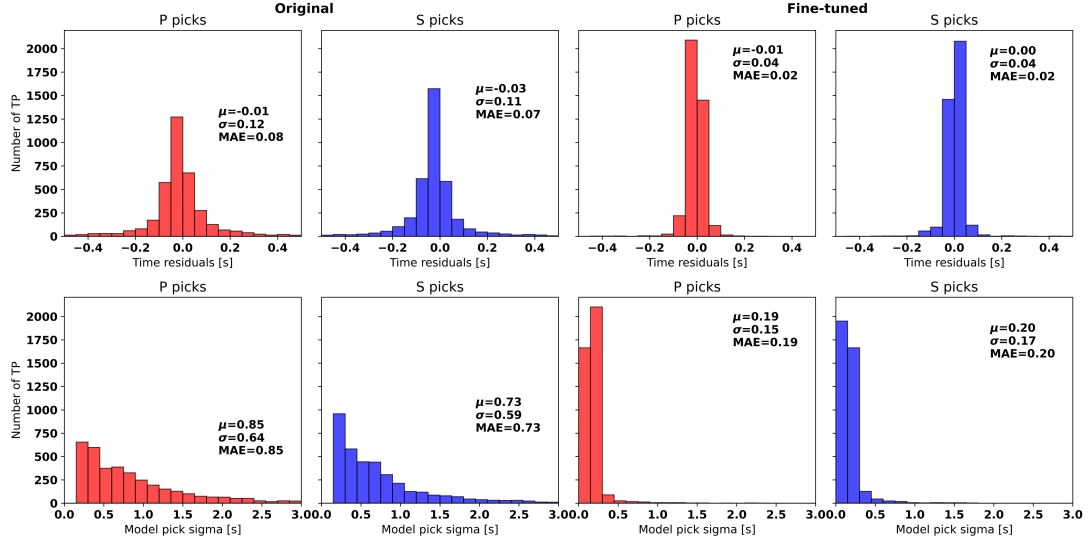


Fig. 8 Comparison of picking arrival time differences (top row) and predicted uncertainty computed from the probability function of a corresponding pick (bottom row) on the test set #1 for two deep-learning models: the original PhaseNO (left) and the fine-tuned PhaseNO (right). The top-row histograms show time residuals for P-wave picks (red) and S-wave picks (blue), defined as the difference between the model-predicted arrivals and the manual labels. Each panel reports the mean (μ), standard deviation (σ), and mean absolute error (MAE) for all true-positive (TP) picks with time residuals below 0.5 s. The bottom-row histograms display the distribution of 1-sigma probability intervals for TPs in each model. Notably, the fine-tuned model's mean residual is closer to zero, and its average uncertainty interval is about three times smaller than that of the original PhaseNO, indicating improved overall picking accuracy.

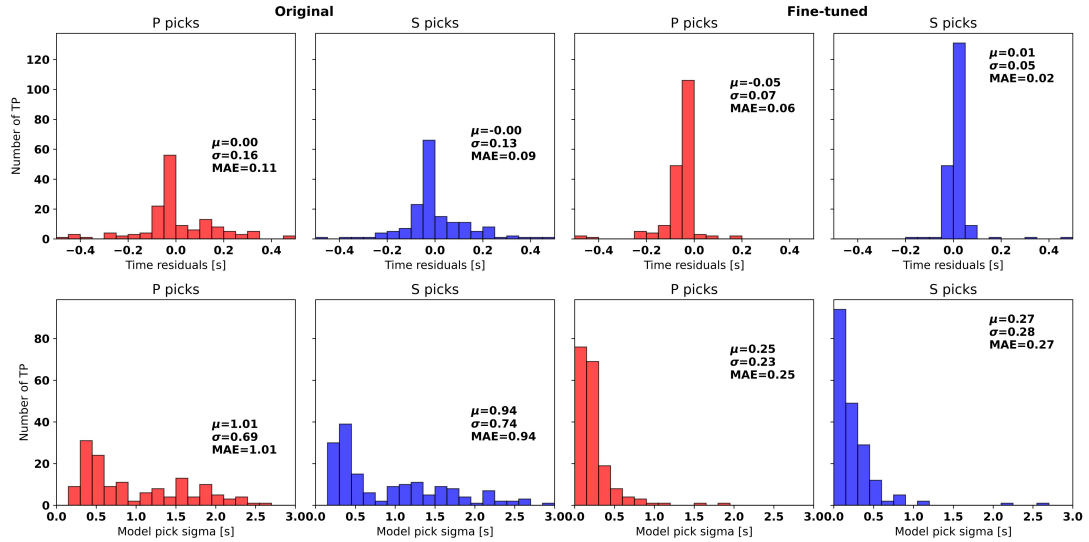


Fig. 9 Comparison of picking arrival time differences (top row) and predicted uncertainty computed from the probability function of a corresponding pick (bottom row) on the test set #2 for two deep-learning models: the original PhaseNO (left) and the fine-tuned PhaseNO (right). The top-row histograms show time residuals for P-wave picks (red) and S-wave picks (blue), defined as the difference between the model-predicted arrivals and the manual labels. Each panel reports the mean (μ), standard deviation (σ), and mean absolute error (MAE) for all true-positive (TP) picks with time residuals below 0.5 s. The bottom-row histograms display the distribution of 1-sigma probability intervals for TPs in each model. Similar to the D1 dataset performance, the fine-tuned model's mean residual is closer to zero, and its average uncertainty interval is about three times smaller than that of the original PhaseNO, indicating improved overall picking accuracy.

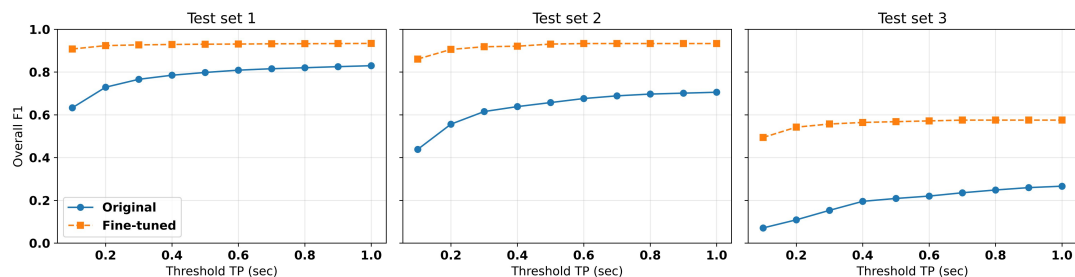


Fig. 10 Sensitivity of overall F1 score to the true-positive time-tolerance threshold for the original and fine-tuned models across the three test sets. For all datasets, the fine-tuned model consistently outperforms the original PhaseNO variant over the full threshold range (0.1–1.0 s). While increasing the tolerance yields a gradual improvement in F1 for both models, the fine-tuned version maintains a substantially higher and more stable performance.

of America **104**(1), 394–409 (2014)

Baker, B., Holt, M.M., Pankow, K.L., Koper, K.D., Farrell, J.: Monitoring the 2020 magna, utah, earthquake sequence with nodal seismometers and machine learning. *Seismological Society of America* **92**(2A), 787–801 (2021)

Chen, G., Li, J.: Cubenet: Array-based seismic phase picking with deep learning. *Seismological Society of America* **93**(5), 2554–2569 (2022)

Chai, C., Maceira, M., Santos-Villalobos, H.J., Venkatakrisnan, S.V., Schoenball, M., Zhu, W., Beroza, G.C., Thurber, C., Team, E.C.: Using a deep neural network and transfer learning to bridge scales for seismic phase picking. *Geophysical Research Letters* **47**(16), 2020–088651 (2020)

Feng, T., Mohanna, S., Meng, L.: Edgephase: A deep learning model for multi-station seismic phase picking. *Geochemistry, Geophysics, Geosystems* **23**(11), 2022–010453 (2022)

Gilmer, J., Schoenholz, S.S., Riley, P.F., Vinyals, O., Dahl, G.E.: Neural message passing for quantum chemistry. In: *International Conference on Machine Learning*, pp. 1263–1272 (2017). PMLR

He, Z., Peng, P., Wang, L., Jiang, Y.: Pickcapsnet: Capsule network for automatic p-wave arrival picking. *IEEE Geoscience and Remote Sensing Letters* **18**(4), 617–621 (2020)

Johnson, S.W., Chambers, D.J., Boltz, M.S., Koper, K.D.: Application of a convolutional

- neural network for seismic phase picking of mining-induced seismicity. *Geophysical journal international* **224**(1), 230–240 (2021)
- Kirschner, D., Howes, N., Daly, C., Mukherjee, J., Li, J.: Detecting p-and s-wave arrivals with a recurrent neural network. In: *SEG International Exposition and Annual Meeting*, pp. 043–119005 (2019). SEG
- Kovachki, N., Li, Z., Liu, B., Azizzadenesheli, K., Bhattacharya, K., Stuart, A., Anandkumar, A.: Neural operator: Learning maps between function spaces with applications to pdes. *Journal of Machine Learning Research* **24**(89), 1–97 (2023)
- Kolar, P., Waheed, U.b., Eisner, L., Matousek, P.: Arrival times by recurrent neural network for induced seismic events from a permanent network. *Frontiers in big Data* **6**, 1174478 (2023)
- Li, Z., Kovachki, N., Azizzadenesheli, K., Liu, B., Bhattacharya, K., Stuart, A., Anandkumar, A.: Fourier neural operator for parametric partial differential equations. *arXiv preprint arXiv:2010.08895* (2020)
- Li, Z., Kovachki, N., Azizzadenesheli, K., Liu, B., Bhattacharya, K., Stuart, A., Anandkumar, A.: Neural operator: Graph kernel network for partial differential equations. *arXiv preprint arXiv:2003.03485* (2020)
- Mousavi, S.M., Ellsworth, W.L., Zhu, W., Chuang, L.Y., Beroza, G.C.: Earthquake transformer—an attentive deep-learning model for simultaneous earthquake detection and phase picking. *Nature communications* **11**(1), 3952 (2020)
- Ross, Z.E., Meier, M.-A., Hauksson, E., Heaton, T.H.: Generalized seismic phase detection with deep learning. *Bulletin of the Seismological Society of America* **108**(5A), 2894–2901 (2018)
- Retailleau, L., Saurel, J.-M., Zhu, W., Satriano, C., Beroza, G.C., Issartel, S., Boissier, P., Team, O., Team, O., *et al.*: A wrapper to use a machine-learning-based algorithm for earthquake monitoring. *Seismological Research Letters* **93**(3), 1673–1682 (2022)
- Shi, P., Meier, M.-A., Villiger, L., Tuinstra, K., Selvadurai, P.A., Lanza, F., Yuan, S., Obermann, A., Mesimeri, M., Münchmeyer, J., *et al.*: From labquakes to megathrusts: Scaling deep learning based pickers over 15 orders of magnitude. *Journal of Geophysical Research: Machine Learning and Computation* **1**(4), 2024–000220 (2024)
- Sun, H., Ross, Z.E., Zhu, W., Azizzadenesheli, K.: Phase neural operator for multi-station picking of seismic arrivals. *Geophysical Research Letters* **50**(24), 2023–106434 (2023)
- Laat, L., Baldares, R.J., Chaves, E.J., Menezes, E.: Oksp: a novel deep learning automatic event detection pipeline for seismic monitoring in costa rica. In: *2021 IEEE 3rd International Conference on BioInspired Processing (BIP)*, pp. 1–6 (2021). IEEE
- Wang, J., Xiao, Z., Liu, C., Zhao, D., Yao, Z.: Deep learning for picking seismic arrival times. *Journal of Geophysical Research: Solid Earth* **124**(7), 6612–6624 (2019)
- Zhu, W., Beroza, G.C.: Phasenet: a deep-neural-network-based seismic arrival-time picking method. *Geophysical Journal International* **216**(1), 261–273 (2019)
- Zhou, Y., Ding, H., Ghosh, A., Ge, Z.: Ai-pal: Self-supervised ai phase picking via rule-based algorithm for generalized earthquake detection. *Journal of Geophysical Research: Solid Earth* **130**(4), 2025–031294 (2025)